

# IMAGINARY CHEMICAL POTENTIAL IN QCD AT FINITE TEMPERATURE

MASSIMO D'ELIA

*Dipartimento di Fisica dell'Università di Genova and INFN, I-16146, Genova, Italy*  
*E-mail: delia@ge.infn.it*

MARIA-PAOLA LOMBARDO

*Istituto Nazionale di Fisica Nucleare, Sezione di Padova, I-35131, Padova, Italy*  
*E-mail: lombardo@pd.infn.it*

After presenting a brief review of how simulations of QCD with imaginary chemical potential can be used to extract physical results, we analyse the phase structure of QCD with four flavours of dynamical fermions in the finite temperature - imaginary chemical potential plane, and discuss perspectives for realistic calculations.

## 1 Introduction

The zero density QCD partition function,  $Z(V, T) = \text{Tr} \left( e^{-\frac{H_{\text{QCD}}}{T}} \right)$ , with  $H_{\text{QCD}}$  the QCD Hamiltonian, can be discretized on an euclidean lattice with finite temporal extent  $\tau = 1/T$

$$Z = \int (\mathcal{D}U \mathcal{D}\psi \mathcal{D}\bar{\psi}) e^{-\beta S_G[U]} e^{-S_F[U, \psi, \bar{\psi}]} = \int (\mathcal{D}U) e^{-\beta S_G[U]} \det M[U] \quad (1)$$

where  $U$  are the gauge link variables and  $\psi$  and  $\bar{\psi}$  the fermionic variables,  $S_G$  is the pure gauge action,  $S_F$  is the fermionic action which can be expressed as a quadratic form in the fermionic fields in terms of the fermionic matrix  $M[U]$ ,  $S_F = \bar{\psi} M[U] \psi$ .

To describe QCD at finite density the grand canonical partition function,  $Z(V, T, \mu) = \text{Tr} \left( e^{-\frac{H_{\text{QCD}} - \mu N}{T}} \right)$ , where  $N = \int d^3x \psi^\dagger \psi$  is the quark number operator, can be used. The correct way to introduce a finite chemical potential  $\mu$  on the lattice <sup>1</sup> is to modify the temporal links appearing in the integrand in Eq. (1) as follows:

$$\begin{aligned} U_t &\rightarrow e^{a\mu} U_t && \text{(forward temporal link)} \\ U_t^\dagger &\rightarrow e^{-a\mu} U_t^\dagger && \text{(backward temporal link) ,} \end{aligned} \quad (2)$$

where  $a$  is the lattice spacing. Whilst  $S_G$  is left invariant by this transformation,  $\det M[U]$  is not and gets a complex phase which makes importance sampling, and therefore standard lattice MonteCarlo simulations, unfeasible.

The situation is different when the chemical potential is purely imaginary. This is implemented on the lattice as described in Eq. (2), but in this case  $U_t \rightarrow e^{ia\mu_I} U_t$ ,  $U_t^\dagger \rightarrow e^{-ia\mu_I} U_t^\dagger$ . This is like adding a constant  $U(1)$  background field to the original theory;  $\det M[U]$  is again real and positive and simulations are as easy as at  $\mu = 0$ .

The question then arises how simulations at imaginary chemical potential may be of any help to get physical interesting information.

One possibility is analytic continuation<sup>2</sup>.  $Z(V, T, \mu)$  is expected to be an analytical even function of  $\mu$  away from phase transitions. For small enough  $\mu$  one can write:

$$\log Z(\mu) = a_0 + a_2\mu^2 + a_4\mu^4 + O(\mu^6) \quad (3)$$

$$\log Z(\mu_I) = a_0 - a_2\mu_I^2 + a_4\mu_I^4 + O(\mu_I^6) . \quad (4)$$

Simulations at small  $\mu_I$  will thus allow a determination of the expansion coefficients for the free energy and, analogously, for other physical quantities, which can be cross-checked with those obtained by standard reweighting techniques<sup>3,4</sup>. This method is expected to be useful in the high temperature regime, where the first coefficients should be sensibly different from zero; moreover the region of interest for present experiments (RHIC, LHC) is that of high temperatures and small chemical potential, with  $\mu/T \sim 0.1$ . This method has been already investigated in the strong coupling regime<sup>2</sup>, in the dimensionally reduced 3-d QCD theory<sup>5</sup>, and in full QCD with two flavours<sup>6</sup>. The Taylor expansion coefficients can also be measured as derivatives with respect to  $\mu$  at  $\mu = 0$ <sup>7,8</sup>.

$Z(V, T, i\mu_I)$  can also be used to reconstruct the canonical partition function  $Z(V, T, n)$  at fixed quark number  $n$ <sup>9</sup>, *i.e.* at fixed density:

$$\begin{aligned} Z(V, T, n) &= \text{Tr} \left( \left( e^{-\frac{H_{\text{QCD}}}{T}} \delta(N - n) \right) \right) = \frac{1}{2\pi} \text{Tr} \left( e^{-\frac{H_{\text{QCD}}}{T}} \int_0^{2\pi} d\theta e^{i\theta(N-n)} \right) \\ &= \frac{1}{2\pi} \int_0^{2\pi} d\theta e^{-i\theta n} Z(V, T, i\theta T) . \end{aligned} \quad (5)$$

As  $n$  grows, the factor  $e^{-i\theta n}$  oscillates more and more rapidly and the error in the numerical integration grows exponentially with  $n$ : this makes the application of the method difficult especially at low temperatures where  $Z(V, T, i\mu_I)$  depends very weakly on  $\mu_I$ . The method has been applied in the 2-d Hubbard model<sup>10</sup>, where  $Z(V, T, n)$  has been reconstructed up to  $n = 6$ .

The phase structure of QCD in the  $T - i\mu_I$  plane is also interesting by its own. Writing for brief  $Z(\theta) \equiv Z(V, T, i\theta T) = \text{Tr} \left( e^{i\theta N} e^{-\frac{H_{\text{QCD}}}{T}} \right)$ ,  $Z(\theta)$  is clearly periodic in  $\theta$  with period  $2\pi$  and a period  $2\pi/3$  is expected in the

confined phase, where only physical states with  $N$  multiple of 3 are present. However it has been shown<sup>9</sup> that  $Z(\theta)$  has always period  $2\pi/3$  for any physical temperature. Moreover the suggestion has been made<sup>9</sup>, based on a calculation in the weak coupling approximation, that discontinuities in the first derivatives of the free energy at  $\theta = 2\pi/3(k+1/2)$  should appear in the high temperature phase. This suggests a very interesting scenario for the phase diagram of QCD in the  $T - i\mu_I$  plane which needs confirmation by lattice calculations.

We have recently started a program of simulations of QCD at finite imaginary chemical potential, with both the aim of determining the phase diagram of QCD in the entire  $T - i\mu_I$  plane, and exploring by analytic continuation the high  $T$  - small real chemical potential region.

We have studied QCD with four degenerate staggered flavours of bare mass  $a \cdot m = 0.05$  on a  $16^4 \times 4$  lattice, where the phase transition is expected at a critical coupling  $\beta_c \simeq 5.04$ <sup>11</sup> (the two flavour case has been studied as well<sup>6</sup>). The algorithm used is the standard HMC  $\Phi$  algorithm. We will present here only a subset of our results and analysis. A complete presentation will appear soon<sup>12</sup>.

## 2 Results

In order to understand the phase structure of the theory, it is very useful to look at the phase of the trace of the Polyakov loop,  $P(\vec{x})$ . Let us parametrize  $P(\vec{x}) \equiv |P(\vec{x})|e^{i\phi}$ , and let  $\langle\phi\rangle$  be the average value of the phase. In the pure gauge theory the average Polyakov loop is non zero only in the deconfined phase, where the center symmetry is spontaneously broken and  $\langle\phi\rangle = 2k\pi/3$ ,  $k = -1, 0, 1$ , *i.e.* the Polyakov loop effective potential is flat in the confined phase and develops three degenerate minima above the critical temperature. In presence of dynamical fermions  $P(\vec{x})$  enters explicitly the fermionic determinant and  $Z_3$  is broken: the effect of the determinant is therefore like that of an external magnetic field which aligns the Polyakov loop along  $\langle\phi\rangle = 0$ . In the high temperature phase the  $Z_3$  degeneracy is lifted:  $\langle\phi\rangle = 0$  is the true vacuum and  $\langle\phi\rangle = \pm 2\pi/3$  are now metastable minima.

When  $\mu_I \neq 0$ , what enters the fermionic determinant is  $P(\vec{x})e^{i\theta}$ ,  $\theta \equiv \mu_I/T$ , instead of  $P(\vec{x})$ . Therefore the determinant now tends to align  $\langle\phi\rangle + \theta$  along zero: its effect is like that of an external magnetic field pointing in the  $\theta$  direction. Hence one expects  $\langle\phi\rangle = -\theta$  at low temperatures; at high temperatures the external magnetic field will still lift the  $Z_3$  degeneracy, but now which is the true vacuum will depend on the value of  $\theta$ . In particular one expects that for  $(k - 1/2) < \frac{3}{2\pi}\theta < (k + 1/2)$  the true vacuum is the one with  $\langle\phi\rangle = 2k\pi/3$  and that  $\theta = 2(k + 1/2)\pi/3$  corresponds to first order phase

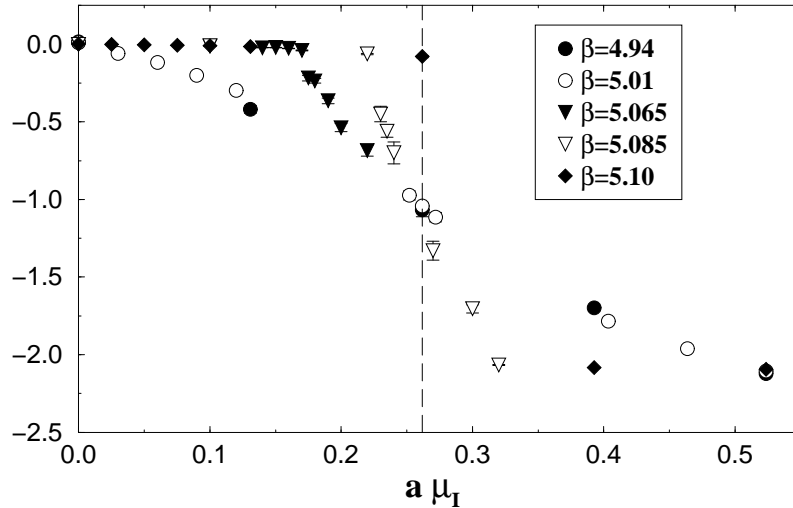


Figure 1. Average value of the Polyakov loop phase as a function of the imaginary chemical potential for different values of  $\beta$ . The vertical dashed line corresponds to  $\theta = \mu_I/T = \pi/3$ .

transitions from one  $Z_3$  sector to the other: this is indeed the prediction of Roberge and Weiss.

In Fig. 1 we report our results for  $\langle\phi\rangle$  versus the imaginary chemical potential for different values of  $\beta$ . Since  $T = 1/(N_t a)$  and  $N_t = 4$  in our case, we have  $\theta = 4a\mu_I$ . For  $\beta = 4.94$  and  $5.01$ , which are below the critical  $\beta$  at  $\mu_I = 0$ ,  $\beta_c(\mu_I = 0) \equiv \beta_c \simeq 5.04$ , one has  $\langle\phi\rangle \simeq -\theta = -4a\mu_I$ , *i.e.*  $\langle\phi\rangle$  is driven continuously by the fermionic determinant. For  $\beta = 5.10$ , which is well above  $\beta_c$  we see that  $\langle\phi\rangle \simeq 0$ , almost independently of  $\mu_I$ , as long as  $\theta < \pi/3$ , while for  $\theta > \pi/3$  there is a sudden change to  $\langle\phi\rangle \simeq -\pi/3$ : we are clearly crossing the Roberge-Weiss phase transition from one  $Z_3$  sector to the other. At intermediate values,  $\beta = 5.065$  and  $5.085$ ,  $\langle\phi\rangle \simeq 0$  until a critical value of  $a\mu_I$ , where it starts moving almost linearly with  $\mu_I$  crossing continuously the  $Z_3$  boundary: in this case there is no Roberge-Weiss phase transition, but there is anyway a critical value of  $\mu_I$  after which  $\langle\phi\rangle$  is no more constrained to be  $\simeq 0$  and can be driven again by  $\theta$ : as we will soon clarify, this critical value of  $\mu_I$  corresponds to the crossing of the chiral critical line, *i.e.* the continuation in the  $T-\mu_I$  plane of the chiral phase transition.

We display our results for the chiral condensate in Fig. 2. We expect a periodicity with period  $2\pi/3$  in terms of  $\theta$ . Moreover  $\langle\bar{\psi}\psi\rangle$ , like the partition function, is an even function of  $\mu_I$ : this, combined with the periodicity, leads to symmetry around all points  $\theta = n\pi/3$ . with  $n$  an integer number, for  $\langle\bar{\psi}\psi\rangle$

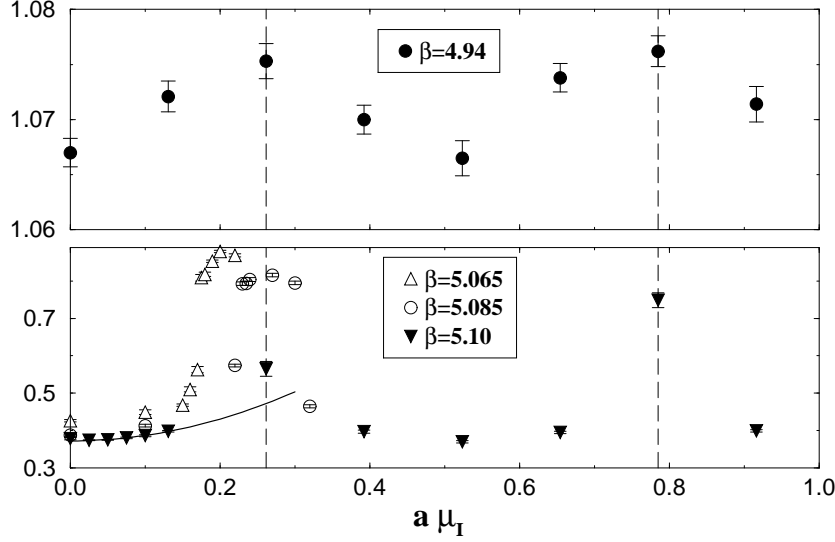


Figure 2. Average value of the chiral condensate as a function of the imaginary chemical potential for different values of  $\beta$ . The vertical dashed lines correspond to  $\theta = \mu_I/T = (2k+1)\pi/3$ . The continuous line in the lower picture is the result of a quadratic fit at small values of  $a\mu_I$  obtained at  $\beta = 5.10$ .

as well as for the partition function itself. For  $\beta < \beta_c$ ,  $\langle \bar{\psi}\psi \rangle$  has a continuous dependence on  $a\mu_I$  with the expected periodicity and symmetries. For  $\beta > \beta_c$  the correct periodicity and symmetries are still observed but the dependence is less trivial. At  $\beta = 5.065$  there is a critical value  $a\mu_I \simeq 0.17$  for which the theory has a transition to a spontaneously broken chiral symmetry phase: we are clearly going through the chiral critical line. The same happens for  $\beta = 5.085$  at  $a\mu_I \simeq 0.22$ : in this case we have proceeded further, observing also the transition back to a chirally restored phase at  $a\mu_I \simeq 0.30$ , which is, correctly, the symmetric point with respect to  $\theta = \pi/3^a$ . At  $\beta = 5.10$  we never cross, when moving in  $\mu_I$ , the chiral critical line, but only the Roberge-Weiss critical lines <sup>b</sup>.

We have also performed runs at fixed  $\mu_I$  and variable  $\beta$  to look for other locations of the chiral line in the  $T-\mu_I$  plane, a detailed summary of all results will be presented elsewhere <sup>12</sup>. We present, in Fig. 3, a sketch of the phase dia-

<sup>a</sup> We notice a discrepancy in the results obtained at the same  $\beta$  by multireweighting techniques <sup>4</sup>, where the same symmetry cannot be observed.

<sup>b</sup> Error bars for the determinations at  $\beta = 5.10$  and on the critical lines ( $\theta = \pi/3$  and  $\theta = \pi$ ) are probably underestimated.

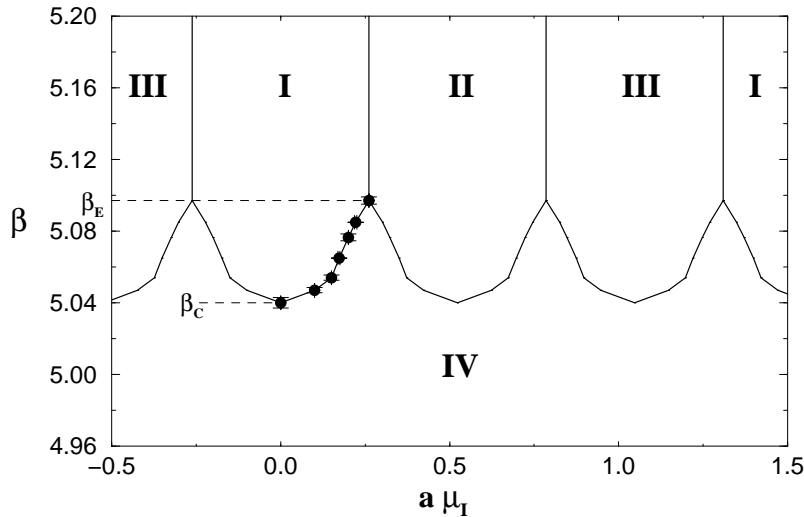


Figure 3. Sketch of the phase diagram in the  $\mu_I$ - $\beta$  plane. The filled circles represents direct determinations of the chiral critical line location from our simulations. The rest of the chiral line has been obtained by interpolation and by exploiting the symmetries of the partition function.

gram in the  $\beta$ - $\mu_I$  plane, as emerges from our data and by exploiting the above mentioned symmetries. We can distinguish a region where chiral symmetry is spontaneously broken (indicated as IV in the figure) and three regions (I, II and III), which correspond to different  $Z_3$  sectors and repeat periodically, where chiral symmetry is restored. The chiral critical line separates region IV from other regions, while the Roberge-Weiss critical lines separate regions I,II and III among themselves. In QCD with 4 staggered flavours,  $am = 0.05$  and  $\mu_I = 0$ , the phase transition is expected to be first order<sup>11</sup>: assuming it continues to be first order also at  $\mu_I \neq 0$ , we expect all the regions to be separated by first order critical lines.

It is interesting to illustrate the determination of the endpoint of the Roberge-Weiss critical line,  $\beta_E = 5.097(2)$ . We have performed a simulation at exactly  $\theta = \pi/3$ : starting thermalization at an high value of  $\beta$  from a zero field configuration we always stay on the border of region I, since on the  $16^3 \times 4$  lattice that we have used it is practically impossible to flip into region II through the critical line. As we decrease  $\beta$ , always staying on the border of region I, we will meet the chiral critical line at  $\beta = \beta_E$ . Various quantities can obviously be considered to signal this transition, but it is interesting to notice that in this case the baryon density can be taken as an exact order parameter. Indeed the baryon density,  $\langle b \rangle = \frac{T}{V} \frac{\partial}{\partial \mu} \ln Z$ , is an odd function of  $\mu$ , being

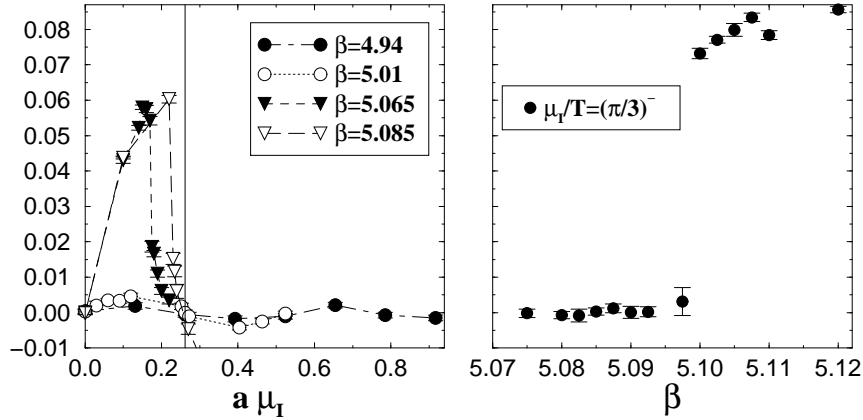


Figure 4. Imaginary part of the baryon density as a function of  $\mu_I$  for different values of  $\beta$  (left-hand side), and as a function of  $\beta$  at  $\theta = \mu_I/T = \frac{\pi}{3}$  (right-hand side).

$Z$  an even function. Therefore, for an imaginary chemical potential,  $\langle b \rangle$  is also purely imaginary and an odd function of  $\mu_I$ . This, combined with the periodicity in  $\mu_I$ , leads to the expectation that  $\langle b \rangle(\theta = \frac{\pi}{3}) = -\langle b \rangle(\theta = \frac{\pi}{3})$ . The last relation clearly implies that  $\langle b \rangle = 0$  at  $\theta = \pi/3$ , unless  $\langle b \rangle$  is not continuous on that point. Thus a non-zero value of  $\langle b \rangle = 0$  at  $\theta = \frac{\pi}{3}$  implies the presence of the Roberge-Weiss critical line. On the right hand side of Fig. 4 the imaginary part of  $\langle b \rangle$  at  $\theta = \frac{\pi}{3}$  is plotted as a function of  $\beta$ : one can clearly see a transition from a zero to a non-zero expectation value, which permits the determination of  $\beta_E$ . We have verified that the transition through  $\beta_E$  is also visible in the chiral condensate: this implies that the Roberge-Weiss critical line ends on the chiral critical line. On the left hand side of Fig. 4 we present instead the imaginary part of  $\langle b \rangle$  as a function of  $\mu_I$  for different values of  $\beta < \beta_E$ : in this case  $\langle b \rangle$  is always zero and continuous at  $\theta = \frac{\pi}{3}$ , but it is interesting to note how it starts developing the discontinuity as  $\beta \rightarrow \beta_E$ .

In order to translate results for  $\beta_c(\mu_I)$  into results for the physical critical temperature,  $T_c(\mu_I)$ , we need the lattice spacing,  $a = a(\beta)$ , in physical units. For instance using the values  $a(5.04) = 0.30(2)$  fm and  $a(5.097) = 0.272(10)$  fm<sup>13</sup> we obtain  $T_c = 164(10)$  MeV and  $T_E = 181(7)$  MeV.

Finally we notice that for high temperatures and away from the critical lines, physical quantities show a clear non-zero dependence on the imaginary chemical potential, which is encouraging in starting the program of fitting the first terms of their Taylor expansion in  $\mu_I$  and performing the analytic continuation to real chemical potential. As an example we have reported, in Fig. 2, the result of a quadratic fit in  $\mu_I$  for the chiral condensate at  $\beta = 5.10$ .

### 3 Summary and discussion

We have clarified the phase structure in the imaginary chemical potential – temperature plane for full QCD with four staggered flavours. In particular we have confirmed the existence of the Roberge Weiss critical lines, located their endpoints and assessed their interplay with the chiral critical lines.

We have checked that data at high temperature and small imaginary chemical potential can be safely fitted by a polynomial, when away from phase transition lines, making the analytic continuation to real  $\mu$  feasible.

The physical interesting region of high temperature and small chemical potential can now be studied by essentially three different techniques: 1) Direct calculations of derivatives; 2) Reweighting; 3) Analytic continuation from imaginary  $\mu$ . Each method has its own merits and limitations, and cross checks among the three approaches should produce reliable results.

### Acknowledgments

This work has been partially supported by MIUR. We thank the computer center of ENEA for providing us with time on their QUADRICS machines.

### References

1. J.B. Kogut *et al.*, *Nucl. Phys. B* **225**, 93 (1983); P. Hasenfratz and F. Karsch, *Phys. Lett. B* **125**, 308 (1983).
2. M.P Lombardo, *Nucl. Phys. B(Proc. Suppl.)* **83**, 375 (2000).
3. I.M. Barbour *et al.*, *Nucl. Phys. B(Proc. Suppl.)* **60A**, 220 (1998).
4. Z. Fodor and S.D. Katz, arXiv:hep-lat/0104001; arXiv:hep-lat/0106002.
5. A. Hart, M. Laine and O. Philipsen, *Nucl. Phys. B* **586**, 443 (2000); *Phys. Lett. B* **505**, 141 (2001).
6. Ph. de Forcrand and O. Philipsen, arXiv:hep-lat/0205016; O. Philipsen, arXiv:hep-lat/0110051.
7. S. Gottlieb *et al.*, *Phys. Rev. D* **38**, 2888 (1988); R.V. Gavai and S. Gupta, arXiv:hep-lat/0202006.
8. C.R. Allton *et al.*, arXiv:hep-lat/0204010; S. Choe *et al.*, *Phys. Rev. D* **65**, 054501 (2002).
9. A. Roberge and N. Weiss, *Nucl. Phys. B* **275**, 734 (1986).
10. M. G. Alford, A. Kapustin, F. Wilczek, *Phys. Rev. D* **59**, 054502 (1999).
11. F.R. Brown *et al.*, *Phys. Lett. B* **251**, 181 (1990).
12. M. D’Elia, M.P. Lombardo, in preparation.
13. B. Alles, M. D’Elia, A. Di Giacomo, *Phys. Lett. B* **483**, 139 (2000).